The Distribution of Sums of Path Gains in the IEEE 802.15.3a UWB Channel Model

Kei Hao and John A. Gubner, *Member, IEEE*

***Abstract*— When multipath arrival times and gains are specified by the IEEE 802.15.3a ultra-wideband (UWB) channel model, formulas are derived for the characteristic function of the sum of gains arriving in a given time window. These formulas are first used to determine structural properties of the corresponding distributions and densities. The formulas are then used to compute the distribution and density functions by numerically inverting the characteristic function. For small time windows, the densities of the path-gain sums are bimodal and therefore highly non-Gaussian.**

***Index Terms*— Cluster process, Saleh–Valenzuela model, point process, shot noise, ultra-wideband.**

I. Introduction

CONSIDER a fading multipath channel in which the kth multipath component arrives at time T_k with corresponding gain G_k. The sum of path gains that arrive in a given time window, say $a \le t \le b$, can be expressed mathematically by the formula

$$\Phi := \sum_k G_k I_{[a,b]}(T_k), \tag{1}$$

where the indicator function $I_{[a,b]}(t) := 1$ if $t \in [a,b]$ and is zero otherwise. Such sums of path gains are important because they approximate the channel coefficients of the tapped-delay-line and virtual-channel models [8], [13] used in the study of direct-sequence systems [11].

Our interest is in the cumulative distribution function (cdf) and probability density function (pdf) of the sum of path gains Φ when the arrival times T_k and gains G_k are specified by the IEEE 802.15.3a ultra-wideband (UWB) multipath model [1], [3], [10].

Under the IEEE UWB multipath model, for very small window sizes; e.g., 5.22 ps implicitly used in the code in [3], the average number of paths for most windows is between 0.01 and 0.1. Hence, there can be no hope of a central-limit-theorem effect making the sum of gains Φ approximately normal. Without this approximation, the required analysis is difficult [14].

Under the IEEE UWB multipath model, we derive formulas for the characteristic function of Φ. These formulas are first used to determine structural properties of the corresponding cdf and pdf. The formulas are then used to compute the cdf and pdf by numerically inverting the characteristic function. Our numerical results show, for time windows of length less than or equal to 1 ns, the densities are bimodal and therefore highly non-Gaussian. For time windows of length 5 ns or more, the densities for windows near the origin are nearly Gaussian.

Manuscript received June 26, 2005; revised February 16, 2006 and June 1, 2006; accepted June 27, 2006. The associate editor coordinating the review of this paper and approving it for publication was Z. Tian.

The authors are with the Department of Electrical and Computer Engineering, University of Wisconsin, Madison, WI 53706–1691 USA (e-mail: khao@wisc.edu, gubner@engr.wisc.edu).

Digital Object Identifier 10.1109/TWC.2007.05438.

II. Statement of Theoretical Results

The key parameters of the IEEE UWB multipath model are the **cluster arrival rate** C, the **ray arrival rate** R, and the **power-delay time constants** τ_0 and s_0. The scale factor Ω_0 is the second moment of a gain that arrives at time zero.

A. Prior Results

For any time window $[a,b]$ with $a \ge 0$, it is shown in [7] that $\mathsf{E}[\Phi] = 0$ and that

$$\begin{aligned}\mathsf{var}(\Phi) = \Omega_0\Big(& I_{[a,b]}(0) + R\zeta(a,b,s_0) + C\zeta(a,b,\tau_0) \\ & + CR\big[\zeta(a,b,s_0)\zeta\big(0,a,s_0\tau_0/(s_0-\tau_0)\big) \\ & + s_0\zeta(a,b,\tau_0) \\ & - s_0\zeta\big(a,b,s_0\tau_0/(s_0-\tau_0)\big)e^{-b/s_0}\big]\Big),\end{aligned} \tag{2}$$

where for any $\theta > 0$,

$$\zeta(a,b,\theta) := \theta[e^{-a/\theta} - e^{-b/\theta}].$$

To consider a time window of width Δ starting at time a, let $b = a + \Delta$, and observe that $\zeta(a, a+\Delta, \mu) = \mu e^{-a/\mu}[1 - e^{-\Delta/\mu}]$. Thus, as a function of a, $\mathsf{var}(\Phi)$ decays exponentially fast in a as the window moves away from the origin.

To gain further insight into the sum of path gains in a time window, we concentrate first on the computation of the characteristic function of Φ, and then we compute the cdf and pdf by inverting the characteristic function numerically.

B. New Results

Let $\Psi(\nu) := \mathsf{E}[e^{j\nu\Phi}]$ denote the characteristic function of Φ, and let $F(x)$ denote the corresponding cdf. Proofs of the following results are given in the Appendix.

Theorem 1: The characteristic function $\Psi(\nu)$ of Φ for time window $[a,b]$ has the product form

$$\Psi(\nu) = \begin{cases} e^{-R\psi_\nu(0)}e^{-CJ(\nu)}, & a > 0, \\ \mathcal{L}_{0,0}(\nu)e^{-R\psi_\nu(0)}e^{-CJ(\nu)}, & a = 0, \end{cases} \tag{3}$$

where the functions $\mathcal{L}_{\tau,s}(\nu)$, $\psi_\nu(\tau)$, and $J(\nu)$ are given in the Appendix by the integral formulas (13), (14), and (18), respectively.

Theorem 2: For $a = 0$, $\lim_{|\nu|\to\infty} \Psi(\nu) = 0$, and the characteristic function $\Psi(\nu)$ is absolutely integrable. Thus the cdf $F(x)$ has a continuous pdf $f(x)$.

Theorem 3: For $a > 0$, the characteristic function $\Psi(\nu)$ has the decomposition $\Psi(\nu) = K_0 + \Psi_1(\nu)$, where the limit $K_0 := \lim_{\nu\to\infty} \Psi(\nu)$ exists and is given by

$$K_0 = e^{-R(b-a)}e^{-C[b-ae^{-R(b-a)}]}, \tag{4}$$

and where $\Psi_1(\nu) := \Psi(\nu) - K_0$ is absolutely integrable. Thus the cdf $F(x)$ has the corresponding decomposition

$$F(x) = K_0 u(x) + F_1(x), \tag{5}$$

where $u(\cdot)$ is the unit step function, and $F_1(x)$ is continuous and has a continuous density, i.e., $F(x)$ has the impulsive pdf $f(x) = K_0\delta(x) + f_1(x)$, where

$$f_1(x) = \frac{1}{2\pi}\int_{-\infty}^{\infty} \Psi_1(\nu)e^{-jx\nu}d\nu$$

is continuous and $\lim_{|x|\to\infty} f_1(x) = 0$.

Since (3) is not available in closed-form and each factor is only available as an integral representation, it was necessary to derive several important properties of $\Psi(\nu)$ in order to prove Theorems 2 and 3. This is done in the Appendix.

The term $K_0u(x)$ in (5) has some important implications. First of all, it shows that the cdf of the sum of path gains in a time window $[a, b]$ with $a > 0$ has a jump at $x = 0$. Second, we have the following result:

Theorem 4: The probability that no path gains fall inside a time window $[a, b]$ with $a > 0$ is the quantity K_0.

Theorem 5: The sums of path gains in nonoverlapping windows are uncorrelated but *statistically dependent*.

Although the characteristic function must be computed numerically, and the cdf is obtained by numerically inverting the characteristic function, this is all quite practical as indicated in Section III.

C. Line-of-Sight and Non-Line-of-Sight Models

According to the IEEE 802.15.3a UWB multipath model, the first path arrives at time zero in line-of-sight (LOS) channel models. Hence, initial windows of the form $[0, b]$ are different from noninitial windows of the form $[a, b]$ with $a > 0$. In the non-line-of-sight (NLOS) channel models, there is no distinction between the case $a = 0$ and $a > 0$.

Our results above are stated for LOS channel models, but they hold for NLOS channels with the following modifications. In NLOS channel models there is no cluster at time zero and there are no subsidiary rays either. Hence, in NLOS models, the first two terms inside the large parentheses in (2) are omitted. Similarly, in (3) and (4) only the rightmost factor in each formula is present; i.e., $\Psi(\nu) = e^{-CJ(\nu)}$ and $K_0 = \exp\{-C[b - ae^{-R(b-a)}]\}$. In particular, while Theorem 2 no longer holds, initial windows are accounted for because for NLOS channels, Theorem 3 extends to the case $a = 0$. Similarly, for NLOS channels, Theorem 4 extends to the case $a = 0$. Theorem 5 holds unchanged for NLOS channels.

III. Numerical Results

We now present numerical examples to illustrate the preceding theorems. For the examples we used the parameters of the channel model CM1 in [3, Table 1] and also in [1, Table II], namely

$$\Omega_0 = 1/[(1 + Rs_0)(1 + C\tau_0)], \quad C = 0.0233, \quad R = 2.5,$$
$$\tau_0 = 7.1, \quad s_0 = 4.3, \quad \sigma^2 = \sigma_1^2 + \sigma_2^2, \quad \sigma_1 = \sigma_2 = 3.3941,$$

where C and R are the cluster and ray arrival rates (in ns^{-1}), τ_0 and s_0 are power-delay time constants (in ns), σ is the standard deviation (in dB) of the path gains, and Ω_0 is a scale factor.

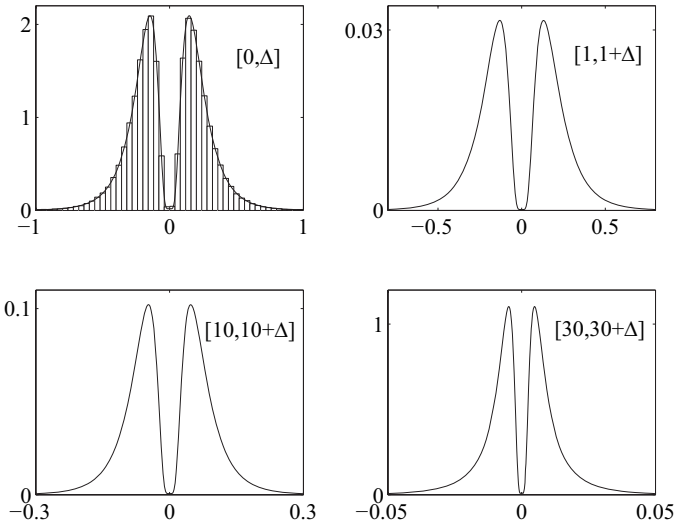

Fig. 1. Density functions of Φ for time windows (in ns) $[0, \Delta]$, $[1, 1 + \Delta]$, $[10, 10 + \Delta]$, and $[30, 30 + \Delta]$, where $\Delta = 0.00522$. The upper-left plot also includes a corresponding histogram obtained via channel simulation. The last three densities contain impulses (not shown) of strengths $K_0 = 0.987$, 0.984, and 0.978, respectively.

A. Computation of the Cdf and Pdf of Φ

In the case of an initial time window ($a = 0$) in LOS channel models, the cdf $F(x)$ is continuous. Hence, we can use the approximation [4]

$$F_{P,D}(x) \approx b_0\Psi(0) + 2\,\mathrm{Re}\sum_{q=0}^{D-1} c_n e^{-jn\pi x/P}, \tag{6}$$

where $c_0 = 0$, $c_n = b_n\Psi(n\pi/P)$ for $n \neq 0$ and

$$b_n := \begin{cases} 1/2, & n = 0, \\ j/n\pi, & n \text{ odd}, \\ 0, & \text{otherwise}. \end{cases}$$

Here, D is the number of terms in the series for the approximation, and P is the approximate support of the corresponding density. For graphical purposes, we approximate the density $f(x)$ by computing divided differences of $F_{P,D}(x)$.

In the case of a noninitial time window ($a > 0$) in LOS channel models or any time window in NLOS channel models, the cdf is not continuous, and the above method does not apply to $F(x)$. However, it *does* apply to $F_1(x)$ in (5). We can thus write $F(x) \approx K_0u(x) + F_{1,P,D}(x)$, where $F_{1,P,D}(x)$ is approximated as in (6) but with $\Psi(\cdot)$ replaced by $\Psi_1(\cdot) = \Psi(\cdot) - K_0$.

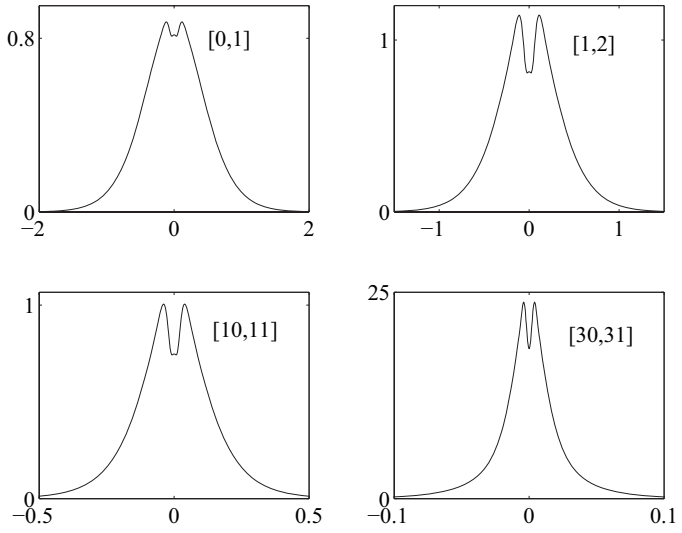

Fig. 2. Density functions of Φ for time windows (in ns) $[0, 1]$, $[1, 2]$, $[10, 11]$, and $[30, 31]$. The last three densities contain impulses (not shown) of strengths $K_0 = 0.079$, 0.065, and 0.042, respectively.

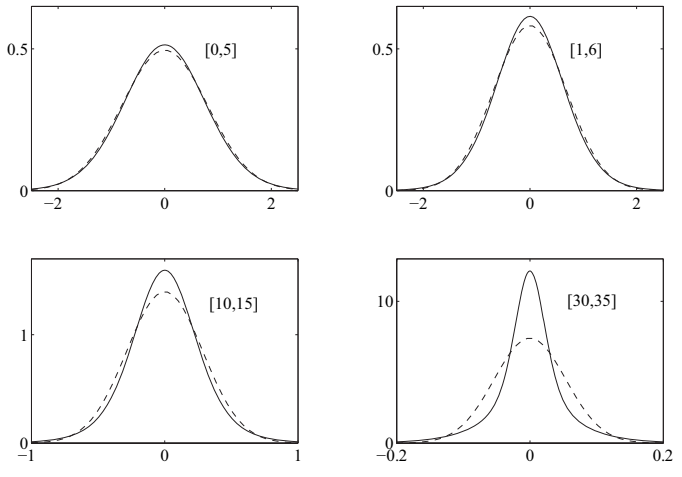

Fig. 3. Density functions of Φ (solid lines) for time windows (in ns) $[0, 5]$, $[1, 6]$, $[10, 15]$, and $[30, 35]$. The last three densities contain impulses (not shown) of strengths $K_0 = 3.42 \times 10^{-6}$, 2.62×10^{-6}, and 1.65×10^{-6}, respectively. The dashed lines are Gaussian densities with mean zero and variance computed using (2).

B. Properties of the Pdf of Φ

Figs. 1–3 show the densities of the sums of gains arriving in various time windows.

As a check on our methods, we compared our numerically computed densities with corresponding histograms obtained from channel simulations. We found excellent agreement, as shown in the upper-left plot of Fig. 1. The other histograms fit equally well, but are omitted to make the figures less cluttered.

We now make a few observations about the figures. First, the densities become more narrow as the window moves away from the origin. This is consistent with the observations about $\mathsf{var}(\Phi)$ made following the formula in (2). Second, for noninitial windows ($a > 0$), the impulse strength K_0 decreases as the window location moves away from the origin. Taking $b = a + \Delta$ in (4) shows that the decay is exponential in a. Third, small window sizes lead to bimodal densities, as shown in Figs. 1 and 2. Fourth, for windows at a fixed starting time, as the width increases, the bimodality decreases, and the densities become more bell shaped. Fifth, windows with unimodal densities become less Gaussian as the window locations move away from the origin.

The foregoing results are for the CM1 channel model, which is a LOS model. We obtained similar results for NLOS channel models.

IV. Conclusions

We have used the accepted IEEE 802.15.3a UWB multipath model to derive formulas to compute the characteristic function of a sum of path gains in LOS and NLOS channel models. We have also derived several structural properties of the corresponding cdf and pdf. We have illustrated these properties in our numerical examples. For initial time windows ($a = 0$) of LOS channel models, the cdf and pdf are continuous functions. For noninitial time windows ($a > 0$) of LOS channel models and any time windows of NLOS channel models, the cdf has a jump discontinuity of height K_0 at $x = 0$. We have shown that K_0 is equal to the probability that no paths fall inside the window. Furthermore, numerical results show that the density functions are very sensitive to the window locations and sizes and can be bimodal and thus highly non-Gaussian.

Appendix

A. Definitions and Notation

If we pair the arrival times T_k and gains G_k in (1) as points (T_k, G_k) in the plane, then we can regard the multipath components as a two-dimensional point process. Furthermore, (1) is then seen to be a special case of the **counting integral**

$$\int_0^\infty \int_{-\infty}^\infty \varphi(s, g)\, N(ds \times dg) := \sum_k \varphi(T_k, G_k), \qquad (7)$$

where $N(\cdot)$ is the **counting measure** on $[0, \infty) \times (-\infty, \infty)$ that puts a unit mass at each point (T_k, G_k), where the arrival times T_k and the path gains G_k are specified by the IEEE 802.15.3a model, and where $\varphi(s, g) = gI_{[a,b]}(s)$.

As described in [1], [3], paths arrive in clusters. The initial cluster arrives at time zero (LOS only), and the remaining clusters arrive at the times of a homogeneous Poisson process whose intensity is the cluster arrival rate C. The noninitial paths of each cluster arrive according to a homogeneous Poisson process starting at the arrival time of the initial path of the cluster and whose intensity is the ray arrival rate R. A path that arrives at time s as a part of a cluster that started at time τ has a gain drawn independently from the density $f_{\tau,s}(\cdot)$ described below.

As pointed out in [7], the foregoing description implies that the counting measure N has the decomposition

$$N(B) = I_{\{(0,G_0)\}}(B) + N_{r0}(B) + N_{\otimes}(B), \quad B \subset \mathbb{R}^2, \qquad (8)$$

where all three terms are independent. In particular, N_{r0} is a two-dimensional Poisson process with intensity

$$\lambda_r(s, g) = Rf_{0,s}(g), \quad s \geq 0, g \in \mathbb{R}. \qquad (9)$$

As a consequence of the independent decomposition in (8), (7) has a corresponding decomposition into three independent terms, which we write as

$$\varphi(0, G_0) + \Phi_{r0} + \Phi_{\otimes}. \tag{10}$$

Note that since N_{r0} is a Poisson process, Φ_{r0} is a Poisson-driven shot-noise random variable. (The foregoing is for LOS models; for NLOS models only the third term in (8) and (10) is present.)

Let $f_{\tau,s}(\cdot)$ denote the density of a path gain arriving at time s that is part of a cluster that started at time τ. Following Saleh and Valenzuela [12, eq. (26)] and Batra *et al*. [1, p. 2126], we assume $f_{\tau,s}(\cdot)$ has second moment[1]

$$\Omega_0 e^{-\tau/\tau_0} e^{-(s-\tau)/s_0}, \tag{11}$$

where τ_0 and s_0 are power-delay time constants and Ω_0 is a scale factor. For the IEEE 802.15.3a model in [1], a $\{\pm 1\}$-valued-Bernoulli$(1/2)$ mixture of lognormal densities is used. This implies that if G has density $f_{\tau,s}(\cdot)$, then $20\log_{10}|G|$ is normal with mean

$$\mu_{\tau,s} := \frac{10}{\ln 10}\Big[\ln \Omega_0 - \tau/\tau_0 - (s-\tau)/s_0 - \Big(\frac{\ln 10}{10}\Big)^2 \frac{\sigma^2}{2}\Big]$$

and variance σ^2. The lognormal mixture density and the lognormal density are related by

$$f_{\tau,s}(x) = \tfrac{1}{2}[f_{|G|,\tau,s}(x) + f_{|G|,\tau,s}(-x)], \tag{12}$$

where $f_{|G|,\tau,s}(\cdot)$ is the lognormal density,

$$f_{|G|,\tau,s}(x) = \frac{20 \exp\Big[\frac{-1}{2\sigma^2}\Big(\frac{20\ln x}{\ln 10} - \mu_{\tau,s}\Big)^2\Big]}{\sqrt{2\pi}\,\sigma x \ln 10}, \quad x > 0,$$

and $f_{|G|,\tau,s}(x) = 0$ otherwise. Because $f_{\tau,s}(\cdot)$ is even, its characteristic function is real and even, and it is easily seen to be

$$\mathcal{L}_{\tau,s}(\nu) := \mathsf{E}_{\tau,s}[e^{j\nu G}] = \int_{-\infty}^{\infty} e^{j\nu g} f_{\tau,s}(g)\, dg, \tag{13}$$

which is just the real part of the characteristic function of a lognormal random variable. By the Riemann–Lebesgue Lemma [2], $\lim_{\nu\to\pm\infty} \mathcal{L}_{\tau,s}(\nu) = 0$. The characteristic function (13) can be evaluated numerically, e.g., using Hermite–Gauss quadrature [5].

For future reference, we put

$$\begin{aligned}\psi_\nu(\tau) &:= \int_{\tau}^{\infty}\int_{-\infty}^{\infty} (1 - e^{j\nu g I_{[a,b]}(s)}) f_{\tau,s}(g)\, dg\, ds \\ &= \begin{cases} \int_{\max(a,\tau)}^{b} 1 - \mathcal{L}_{\tau,s}(\nu)\, ds, & \tau \le b, \\ 0, & \tau > b. \end{cases}\end{aligned} \tag{14}$$

Since the range of integration is finite, the integral can be computed using Legendre–Gauss quadrature. Furthermore,

$$\lim_{\nu\to\infty} \psi_\nu(\tau) = \begin{cases} 0, & \tau > b, \\ b - a, & \tau < a, \\ b - \tau, & a \le \tau \le b. \end{cases}$$

[1]This is in contrast to [1] and [12]. Their ray processes were defined by taking Poisson processes starting at time zero and then translating them by the arrival time of the initial path in the cluster. The two constructions are equivalent provided we adjust the definition of $f_{\tau,s}(\cdot)$. This is done in (11) where we use $s - \tau$; [1] and [12] would use only s.

B. Preliminary Results

The following results are used to prove the theorems stated in Section II-B.

Lemma 6: Let $f \in L^1[0,\infty)$, and put

$$\zeta(\nu) := \int_0^{\infty} e^{j\nu x} f(x)\, dx.$$

If $f' \in L^1[0,\infty)$ and if $f(0) = f(\infty) = 0$, then

$$\lim_{\nu\to\infty} j\nu\zeta(\nu) = 0.$$

Proof: Use integration by parts to write

$$\zeta(\nu) = \frac{1}{j\nu}\int_0^{\infty} e^{j\nu x} f'(x)\, dx.$$

Then multiply through by $j\nu$ and apply the Riemann–Lebesgue Lemma. □

Corollary 7: If the hypotheses of the Lemma 6 hold not only for $f(x)$, but for $f^{(k)}(x)$ for $k = 1, \ldots, m-1$, then

$$(j\nu)^m \zeta(\nu) = \int_0^{\infty} e^{j\nu x} f^{(m)}(x)\, dx \to 0, \quad \text{as} \quad \nu \to \infty.$$

Furthermore, since $f^{(m)} \in L^1$, the above integral is bounded, say by B, and we can write $|\zeta(\nu)| \le B/|\nu|^m$.

Theorem 8: The characteristic function of a lognormal random variable is absolutely integrable.

Proof: Apply Corollary 7 to the lognormal density $f_{|G|,\tau,s}(x)$ with $m = 2$. This shows that the lognormal characteristic function is bounded by $B/|\nu|^2$, which is integrable. □

Lemma 9: The characteristic function of the lognormal mixture random variable is absolutely integrable.

Proof: By (12), $\mathcal{L}_{\tau,s}(\nu) = [\zeta(\nu) + \zeta^*(\nu)]/2$ is absolutely integrable by Theorem 8. □

C. Proofs of Theorems Stated in Section II-B.

Proof of Theorem 1. On account of the independent decomposition in (10), the characteristic function of Φ in (1) factors into

$$\Psi(\nu) := \mathsf{E}[e^{j\nu\Phi}] = \mathsf{E}[e^{j\nu\varphi(0,G_0)}]\mathsf{E}[e^{j\nu\Phi_{r0}}]\mathsf{E}[e^{j\nu\Phi_{\otimes}}]. \tag{15}$$

For the problem we are considering, $\varphi(0, G_0) = I_{[a,b]}(0)G_0$, where G_0 has the lognormal mixture density $f_{0,0}(\cdot)$. Since $I_{[a,b]}(0) = 1 \Leftrightarrow a = 0$, windows that include the origin are different from all other windows. If $a = 0$, then $\mathsf{E}[e^{j\nu\varphi(0,G_0)}] = \mathcal{L}_{0,0}(\nu)$ which is given by (13) with $\tau = s = 0$.

Since Φ_{r0} is a shot-noise random variable driven by a two-dimensional Poisson process with intensity function (9), the second factor in (15) is [9]

$$\exp\Big[\int_0^{\infty}\int_{-\infty}^{\infty} [e^{j\nu\varphi(s,g)} - 1] R f_{0,s}(g)\, dg\, ds\Big],$$

where $\varphi(s,g) := gI_{[a,b]}(s)$. It is easy to see that

$$\mathsf{E}[e^{j\nu\Phi_{r0}}] = e^{-R\psi_\nu(0)}. \tag{16}$$

The third factor in (15) can be computed using the smoothing properties of conditional expectation in a similar manner to that carried out in [6, Appendix]. The result is that

$$\mathsf{E}[e^{j\nu\Phi_{\otimes}}] = e^{-CJ(\nu)}, \tag{17}$$

where

$$J(\nu) := \int_0^\infty \int_{-\infty}^\infty [1 - e^{k_\nu(\tau,\gamma)}] f_{\tau,\tau}(\gamma)\, d\gamma\, d\tau, \tag{18}$$

and

$$k_\nu(\tau,\gamma) := j\nu\gamma I_{[a,b]}(\tau) - R\psi_\nu(\tau).$$

We can thus write

$$\begin{aligned} J(\nu) &= \int_0^\infty 1 - \mathsf{E}_{\tau,\tau}[e^{j\nu\Gamma I_{[a,b]}(\tau)}] e^{-R\psi_\nu(\tau)}\, d\tau \\ &= \int_0^a 1 - e^{-R\psi_\nu(\tau)}\, d\tau + \int_a^b 1 - \mathcal{L}_{\tau,\tau}(\nu) e^{-R\psi_\nu(\tau)}\, d\tau, \end{aligned}$$

where Γ is a generic lognormal mixture random variable with the density function $f_{\tau,\tau}(\cdot)$. □

Proof of Theorem 2. From (15), (16), and (17),

$$\Psi(v) = \mathcal{L}_{0,0}(\nu) e^{-R\psi_\nu(0)} e^{-CJ(\nu)}.$$

Since the second and the third factors are bounded by 1, $|\Psi(v)| \le \mathcal{L}_{0,0}(\nu)$, which is absolutely integrable by Lemma 9. □

Proof of Theorem 3. The formula for K_0 in (4) is established later in Theorem 10. The rest of the proof is as follows. Let $\alpha(\nu) = R\psi_\nu(0) + CJ(\nu)$. Then $\Psi_1(\nu)$ can be written as

$$\int_{-\infty}^\infty |e^{-\alpha(\nu)} - K_0| d\nu.$$

Since the integrand is an even function, it is sufficient to prove that the integral from zero to infinity is finite. We divide the integral into two parts,

$$\int_0^{\nu_0} |e^{-\alpha(\nu)} - K_0| d\nu + \int_{\nu_0}^\infty |e^{-\alpha(\nu)} - K_0| d\nu.$$

The first integral is finite because the integrand is bounded. We need to prove that the second integral is also finite. We compare that integrand with $1/(\nu^p)$ for $p > 1$, i.e., we study

$$\lim_{\nu\to\infty} \frac{e^{-\alpha(\nu)} - K_0}{1/(\nu^p)}.$$

If the quotient converges to zero, it implies the second integral is finite. We cannot compute the limit directly because the numerator and the denominator both converge to zero. Thus, we apply l'Hôpital's rule and consider

$$\lim_{\nu\to\infty} \frac{e^{-\alpha(\nu)}\alpha'(\nu)}{p/(\nu^{p+1})}.$$

Since $\alpha(\nu)$ is bounded, it is sufficient to prove that the first derivative of $\alpha(\nu)$ over $1/\nu^{p+1}$ converges. From the definition of $\alpha(\nu)$,

$$\alpha'(\nu) = R\psi'_\nu(0) + CJ'(\nu). \tag{19}$$

From (14) and (13),

$$\psi'_\nu(0) = -\int_a^b \int_{-\infty}^\infty e^{j\nu g} j g f_{\tau,s}(g)\, dg\, ds. \tag{20}$$

Now observe that

$$\begin{aligned} &\lim_{\nu\to\infty} \psi'_\nu(0)\nu^{p+1} \\ &\quad = -\int_a^b \lim_{\nu\to\infty} \left(\nu^{p+1} \int_{-\infty}^\infty e^{j\nu g} j g f_{\tau,s}(g) dg \right) ds, \end{aligned}$$

where we have appealed to the dominated convergence theorem [2]. Letting $p = 2$, we can apply Corollary 7 with $m = 3$ to the function $g f_{\tau,s}(g)$ and conclude that $\lim_{\nu\to\infty} \psi'_\nu(0)\nu^{p+1} = 0$.

A similar analysis of the second term of (19), ignoring the constant factor, leads to

$$\begin{aligned} &\lim_{\nu\to\infty} \nu^{p+1} J'(\nu) \\ &\quad = -\int_a^b \lim_{\nu\to\infty} \left(e^{-R\psi_\nu(\tau)} \nu^{p+1} \int_{-\infty}^\infty e^{j\nu\gamma} j\gamma f_{\tau,\tau}(\gamma) d\gamma \right) d\tau \\ &\qquad + \int_0^a \lim_{\nu\to\infty} \left(e^{-R\psi_\nu(\tau)} \nu^{p+1} R\psi'_\nu(\tau) \right) d\tau \\ &\qquad + \int_a^b \lim_{\nu\to\infty} \Bigg(e^{-R\psi_\nu(\tau)} \nu^{p+1} R\psi'_\nu(\tau) \\ &\qquad\qquad \cdot \int_{-\infty}^\infty e^{j\nu\gamma} f_{\tau,\tau}(\gamma) d\gamma \Bigg) d\tau. \end{aligned}$$

Since $e^{-R\psi_\nu(\tau)}$ is bounded, and the inner integral of the third term is just the characteristic function of the lognormal mixture random variable and its limit is zero, it can be proved that all three terms converge to zero using the same steps. □

Proof of Theorem 4. If we put $\varphi(s,g) = I_{[a,b]}(s)$, then the counting integral in (7) counts the number paths in the interval $[a,b]$ with $a > 0$. Let N^{ab} denote the number of paths in the interval $[a,b]$. It follows from the independent decomposition in (8) with $B = [a,b] \times \mathbb{R}$ that $N^{ab} = N^{ab}_{r0} + N^{ab}_{\otimes}$ where N^{ab}_{r0} and $N^{ab}_{\otimes}$ are independent. Then the probability generating function is given by

$$G^{ab}(z) = \mathsf{E}[z^{N^{ab}}] = \mathsf{E}[z^{N^{ab}_{r0}}] \mathsf{E}[z^{N^{ab}_{\otimes}}].$$

Since N^{ab}_{r0} is a Poisson random variable, its probability generating function is given by [9]

$$\mathsf{E}[z^{N^{ab}_{r0}}] = e^{-R(b-a)(1-z)}.$$

The second factor can be computed using the smoothing properties of conditional expectation in a similar manner to that carried out in [6, Appendix]. The result is that

$$\mathsf{E}[z^{N^{ab}_{\otimes}}] = e^{-Cq(z)},$$

where

$$q(z) := \int_0^\infty \int_{-\infty}^\infty [1 - z^{I_{[a,b]}(\tau)} e^{\beta_z(\tau,\gamma)}] f_{\tau,\tau}(\gamma)\, d\gamma\, d\tau,$$

and

$$\beta_z(\tau,\gamma) := -R(1-z) \int_\tau^\infty I_{[a,b]}(s) ds.$$

Since this does not depend on γ, we can write

$$\begin{aligned} q(z) &= a[1 - e^{-R(b-a)(1-z)}] \\ &\quad + \int_a^b 1 - z e^{-R(1-z)\int_\tau^\infty I_{[a,b]}(s) ds}\, d\tau. \end{aligned}$$

Then the probability that no path gains fall in the interval can be computed as

$$\mathsf{P}(N^{ab}=0)=G^{ab}(0)=e^{-R(b-a)}e^{-C[b-ae^{-R(b-a)}]}. \quad \square$$

Proof of Theorem 5. The fact that sums of path gains in nonoverlapping windows are uncorrelated was proved in [7]. To prove they are statistically dependent, we proceed as follows. Let $0 \le a < b \le c < d$ and put $B_1 := [a,b]$ and $B_2 := [c,d]$. Let $\Psi_B(\nu)$ be the characteristic function of Φ with $\varphi(s,g)=gI_B(s)$, where $B=B_1 \cup B_2$. Then it is easy to verify that $\Psi_B(\nu) \neq \Psi_{B_1}(\nu)\Psi_{B_2}(\nu)$, where $\Psi_{B_1}(\nu)$ and $\Psi_{B_2}(\nu)$ are the characteristic functions of Φ with $\varphi(s,g)=gI_{B_1}(s)$ and $\varphi(s,g)=gI_{B_2}(s)$ respectively. $\square$

Theorem 10: The characteristic function $\Psi(\nu)$ is a real and even function of ν, and

$$\lim_{\nu\to\infty}\Psi(\nu)=\begin{cases}0, & a=0,\\ e^{-C[b-ae^{-R(b-a)}]}e^{-R(b-a)}, & a>0.\end{cases}$$

Proof: We have that the characteristic function is given by (3). Since $\mathcal{L}_{\tau,s}(\nu)$ is a real and even function of ν, it can be shown that $\psi_\nu(\tau)$ is also a real and even function. Thus, the factor $e^{-R\psi_\nu(\tau)}$ is a real and even function. Similarly, since the integrands of $J(\nu)$ are real and even, $J(\nu)$ is also real and even. Thus, $e^{-CJ(\nu)}$ is real and even. By the dominated convergence theorem, the integrals and the limits of (14), (16), and (17) can be interchanged. Then it is easy to verify that

$$\lim_{\nu\to\infty}e^{-R\psi_\nu(\tau)}=e^{-R(b-a)}$$

and

$$\lim_{\nu\to\infty}e^{-CJ(\nu)}=e^{-C[b-ae^{-R(b-a)}]}.$$

If $a=0$, then $\mathcal{L}_{0,0}(\nu)$ converges to zero by the Riemann–Lebesgue Lemma. $\square$

ACKNOWLEDGMENT

The authors thank the anonymous reviewers for their comments, which were very helpful in improving the paper.

REFERENCES

[1] A. Batra, J. Balakrishnan, G. R. Aiello, J. R. Foerster, and A. Dabak, "Design of a multiband OFDM system for realistic UWB channel environments," *IEEE Trans. Microw. Theory Tech.*, vol. 52, no. 9, pp. 2123–2138, Sept. 2004.

[2] P. Billingsley, *Probability and Measure*. New York: Wiley, 1979.

[3] J. Foerster, Ed., "Channel modeling sub-committee report final," IEEE, Document IEEE P802.15-02/490r1-SG3a, 2003.

[4] J. A. Gubner, "Computation of shot–noise probability distributions and densities," *SIAM J. Sci. Comput.*, vol. 17, no. 3, pp. 750–761, May 1996.

[5] J. A. Gubner, "A new formula for lognormal characteristic functions," *IEEE Trans. Veh. Technol.*, vol. 55, no. 5, pp. 1668–1671, Sept. 2006.

[6] J. A. Gubner and K. Hao, "A computable formula for the average bit-error probability as a function of window size for the IEEE 802.15.3a UWB channel model," *IEEE Trans. Microw. Theory Tech.*, vol. 54, no. 4, pp. 1762–1768, Apr. 2006.

[7] J. A. Gubner and K. Hao, "The IEEE 802.15.3a UWB channel model as a two-dimensional augmented cluster process," submitted for publication.

[8] H. Hashemi, "Impulse response modeling of indoor radio propagation channels," *IEEE J. Sel. Areas Commun.*, vol. 11, no. 7, pp. 967–978, Sept. 1993.

[9] J. F. C. Kingman, *Poisson Processes*. Oxford, UK: Clarendon, 1993.

[10] A. F. Molisch, J. R. Foerster, and M. Pendergrass, "Channel models for ultra-wideband personal area networks," *IEEE Wireless Commun.*, vol. 10, no. 6, pp. 14–21, Dec. 2003.

[11] J. G. Proakis, *Digital Communications, Fourth Edition*. Boston: McGraw-Hill, 2001.

[12] A. A. M. Saleh and R. Valenzuela, "A statistical model for indoor multipath propagation," *IEEE J. Sel. Areas Commun.*, vol. 5, no. 2, pp. 128–137, Feb. 1987.

[13] A. M. Sayeed and B. Aazhang, "Joint multipath-Doppler diversity in mobile wireless communications," *IEEE Trans. Commun.*, vol. 47, pp. 123–132, Jan. 1999.

[14] J. Zhang, R. A. Kennedy, and T. D. Abhayapala, "Performance of RAKE reception for ultra wideband signals in a lognormal fading channel," in *Proc. 2003 Int. Workshop on Ultra Wideband Systems, IWUWBS'2003*.